Neutron Reflectivity of an Adsorbed Water-Soluble Block Copolymer: A Surface Transition to Micelle-like Aggregates at the Air/Water Interface

S. W. An, T. J. Su, and R. K. Thomas*

Physical and Theoretical Chemistry Laboratory, South Parks Road, Oxford OX1 3QZ, U.K.

F. L. Baines, N. C. Billingham, and S. P. Armes

School of Chemistry, Physics and Environmental Science, University of Sussex, Falmer, Brighton BN1 9QJ, U.K.

J. Penfold

ISIS, CCLRC, Chilton, Didcot, Oxon. OX11 0QX, U.K.

Received: April 14, 1997; In Final Form: November 3, 1997[⊗]

We describe neutron reflectivity measurements on layers of poly(2-(dimethylamino)ethyl methacrylate-*block*-methyl methacrylate) copolymer (poly(DMAEMA-*b*-MMA)) (70 mol % DMAEMA, $M_n = 10k$) adsorbed at the air/water interface. Measurements of the partially deuterated copolymer on null reflecting water give the adsorption isotherm and show that there is a surface phase transition from a layer about 20 Å thick to one about 40 Å thick. The concentration of polymer at which the phase transition occurs is close to that at which micellar aggregation in the bulk solution also occurs. Using two other isotopic compositions, the structure of the layer above and below the phase transition has been determined. At low concentration, the two blocks of the copolymer are approximately uniformly distributed in the direction normal to the interface and the layer is partially immersed in water. At high concentrations, the adsorbed layer has a cross-sectional structure resembling that expected for a micelle with the majority of the more hydrophobic MMA residues forming the core. The outer layers, comprising predominantly DMAEMA residues, are not equivalent, being much more highly extended on the aqueous side of the interface.

Introduction

There has been considerable recent interest in the self-assembly of amphiphilic copolymers both in bulk solution and at interfaces. In part this stems from the realization that a very wide range of behavior can be expected and generated, which makes these systems theoretically interesting and opens up a large range of practical applications, and in part because several new experimental techniques have recently emerged, which are capable of probing the structure of aggregates in bulk or at interfaces. The class of diblock copolymers where one block is a polyelectrolyte (block polyelectrolytes) and the other block is hydrophobic are particularly interesting because on one hand they are amphiphilic with respect to water and oil, which is where the widest range of possible technical application can be found, and on the other hand because they present some serious theoretical challenges.

On the experimental side block polyelectrolytes at interfaces have mainly been studied as spread monolayers and, for example, Eisenberg and co-workers[1−4] have demonstrated that there is quite a menagerie of aggregate types, starfish, jellyfish, etc. In these systems there is a strongly hydrophobic block that anchors the polymer to the surface, and the structural variations then mainly stem from the variable behavior of the polyelectrolyte, whose hydrophobicity may be altered by chemical modification (e.g., different length hydrocarbon side chains on a quaternary nitrogen group) or by charge variation (e.g., weak polyelectrolyte[5]). Such systems conform to the models used in most theoretical treatments where there is a strongly hydrophobic anchor or buoy, and then the problem becomes one of how to handle a possibly variable charge on the polyelectrolyte and the balancing of the polyelectrolyte conformation with the elastic energy of the buoy.[6,7] Systems of practical interest, such as those used in emulsion polymerization, wetting, and colloid stabilization, differ from this idealized model in that the hydrophilic/hydrophobic balance is more delicately poised (see e.g., ref 8). This may just be a consequence of the fact that many of the practical uses require water solubility. Then the situation is usually either that each of the components is both water soluble and surface active, but to varying degrees, or that the fraction of water-insoluble material is small enough that the overall copolymer is water-soluble. Under these circumstances it is not so obvious that the traditional anchored polymer chain will be the appropriate starting point for understanding their interfacial behavior.

Our main interest is in the development of water-soluble block copolymers that might be more effective surface-active agents than traditional small-molecule surfactants in a number of fields. For these compounds there seems to be an almost endless range of choice of adjustment of the hydrophilic/lipophilic balance, and it is therefore essential to be able to understand what factors affect the interfacial behavior at a deeper level than hitherto available. In this paper we use neutron reflectivity to study the structure of equilibrium layers of the block polyelectrolyte poly(2-(dimethylamino)ethyl methacrylate-*block*-methyl meth-

[⊗] Abstract published in *Advance ACS Abstracts,* December 15, 1997.

S1089-5647(97)01277-7 CCC: $15.00
Published on Web 01/08/1998

acrylate) (DMAEMA-*b*-MMA) adsorbed at the air/water interface.

Neutron and X-ray reflectivity are powerful new techniques for investigating the air−liquid interface and are increasingly being applied to polymer layers, although there have been relatively few applications to block copolymer layers. Neutron reflection has been used to study spread layers of poly(methyl methacrylate-*b*-ethylene oxide)[9−12] and maleic anhydride−styrene copolymers.[13] Neutron reflection studies on soluble copolymers at the liquid−liquid interface have been made by Phipps et al.[14] and at the air−liquid by Dai et al.[15,16] and Kent et al.,[17] who have respectively studied block copolymers adsorbed at the air−toluene and air−ethyl benzoate interfaces. Neutron and X-ray reflectivity have been used in parallel to study equilibrium monolayers of diblock poly(2-(dimethylamino)ethyl methacrylate-*b*-*n*-butyl methacrylate) at the air/water interface.[18] The most thorough study to date has been by Li et al. who used X-ray specular and off-specular reflectivity to show that poly(styrene-*b*-alkylvinylpyridinium iodide) forms an array of two-dimensional micelles when spread on the surface of water.[3]

Experimental Details

The poly(DMAEMA-*b*-MMA) block copolymer was prepared by group transfer polymerization at 298 K using 1-methoxy-2-methyl-1-(trimethylsiloxy)propene as initiator and tetrabutylammonium dibenzoate catalyst via sequential monomer addition, the DMAEMA being polymerized first.[19,20] ^{1}H NMR spectroscopy and CHN microanalyses indicated an MMA content of 30 mol %. Two copolymer isomers were prepared with the MMA protonated and deuterated (designated hMMA and dMMA). Gel permeation chromatography (tetrahydrofuran eluent; refractive index detector; polystyrene standards) showed that both isotopic block copolymers had narrow unimodal distributions with M_n of 10 000 and 10 600, M_w/M_ns of 1.11 and 1.09, for the poly(DMAEMA-*b*-dMMA) and poly(DMAEMA-*b*-hMMA), respectively.

All the glassware and PTFE troughs were cleaned by soaking them in alkaline detergent overnight and then rinsing several times with ultrapure water (Elgastat UHQ, Elga, U.K.). The solutions were made by dissolving first in methanol and then diluting with water to reach a final methanol concentration of 4 vol %. The pH of the solutions was adjusted using hydrochloric acid and maintained constant during the measurements by keeping the samples under a nitrogen or argon atmosphere. For the neutron measurements D_2O and methanol-d_4 were used as received from Aldrich.

The surface tension of the aqueous copolymer solutions was determined on a Krüss K10T digital tensiometer using the du Noüy ring method with a Pt/Ir ring. The surfaces of solutions of this kind often show time effects, and all measurements were therefore made after the solution had stood for 10−30 min, the longer time being used only if necessary. Before each measurement, the ring was rinsed with pure water and flamed to remove contaminants. The temperature was maintained at 298 ± 0.2 K.

The neutron reflection measurements were carried out on the reflectometers CRISP and SURF at Rutherford Appleton Laboratory (Didcot, U.K.). These instruments and the procedure for making the measurements have been fully described elsewhere.[21,22] In both instruments a polychromatic neutron beam is reflected from the sample at a fixed angle of incidence. Two angles of incidence were used, 0.8° and 1.5°. The neutrons specularly reflected from the sample are detected by a single detector and their wavelengths analyzed by time-of-flight, the reflectivity being determined by the ratio of the reflected neutrons at each wavelength to the number incident on the sample. The neutron reflectivity is measured as a function of momentum transfer κ (=$(4\pi \sin \theta)\ \lambda$, where θ is the glancing angle of incidence and λ the wavelength of the neutrons). The reflection intensities were calibrated with respect to pure D_2O. Incoherent scattering from the bulk solution gives rise to a background, which was determined by measurement of the signal out to large values of κ. This background was assumed to be flat, which has been shown to be approximately valid, provided any small-angle scattering from the bulk solution is small.[23] Although there is the possibility of micellization of the copolymer, the concentrations studied were too low to give significant small-angle scattering.

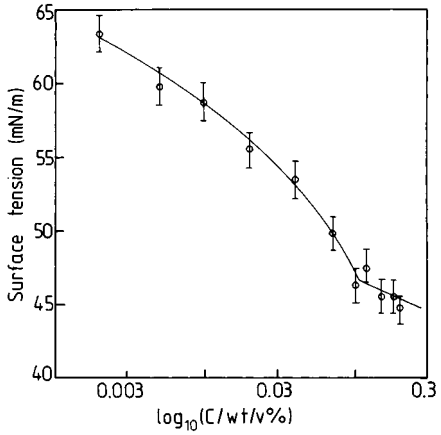

Figure 1. Surface tension of poly(DMAEMA-*b*-MMA) as a function of copolymer concentration at pH = 7.5. The solid lines are for guidance.

Results and Discussion

(a) Surface Tension. Figure 1 shows the variation of surface tension with copolymer concentration of the diblock copolymer in aqueous solution at 298 K and a pH of 7.5 (the natural pH of the copolymer solution in this concentration range is about 8.5). The surface tension decreases to a limiting value of 45−46 mN m^{-1} as the copolymer concentration increases, and this tension is reached at a concentration between 0.1 and 0.2 wt %. This behavior is normally taken to indicate micellization, but it is difficult to extract an accurate value of the cmc because of the relatively large errors in the surface tension measurements of this type of solution. Up to the limiting value of the surface tension a plot of γ against ln c shows an increase in the magnitude of the gradient, which qualitatively corresponds to an increase in surface coverage using the simplest form of the Gibbs equation. We have discussed the application of the Gibbs equation to polymers of this kind and shown that there are major problems in applying it, largely because the degree of ionization, and hence the prefactor in the equation, is not known.[18] We return to this point below after presenting the reflectivity results.

(b) Specular Reflection. The most direct way of examining both composition and structure of a monolayer at the air/water interface is to measure the reflectivity of the partially deuterated solute in null reflecting water (NRW). NRW consists of about 10% D_2O in H_2O and has a neutron refractive index identical with that of air. For a deuterated solute at low concentration there is then no reflected signal unless the solute is adsorbed at the interface. Figure 2 shows a set of reflectivity profiles at different concentrations of poly(DMAEMA-*b*-dMMA) in NRW

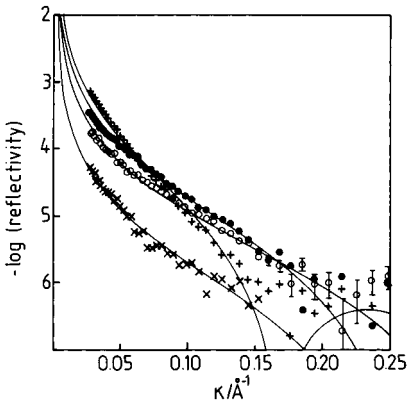

Figure 2. Neutron reflectivity profiles of poly(DMAEMA-*b*-dMMA) in NRW at different concentrations at pH = 7.5. The continuous lines are the best fits using a single-layer model whose parameters are given in Table 2. The bulk concentrations are (+) 0.2, (●) 0.1, (○) 0.04, and (×) 0.02 wt %.

(the 4% methanol in the solution was also adjusted to give zero reflectivity). In these contrast conditions the reflected signal is entirely from the adsorbed copolymer layer.

The simplest analysis of neutron reflection is via the optical matrix method.[24] The refractive index profile of the surface layer normal to the surface is divided into a number of uniform layers, and the Fresnel reflection and transmission coefficients are calculated for each interface and combined to give the total reflectivity from the composite surface layer. The refractive index, n, of a layer is related to its scattering length density, ρ, by

$$n = 1 - (\lambda^2/2\pi)\rho \quad (1)$$

where the scattering-length density is given by

$$\rho = \sum n_i b_i \quad (2)$$

where n_i is the number density of an atomic species i and b_i its empirically determined scattering length. The analysis procedure is then to guess a model for the layer, to compare the calculated and observed reflectivities, and to iterate the process to obtain a satisfactory fit. Unless there are special reasons for believing that the system can be divided into a specified number of layers, the minimum number required to fit the data should be used. The simplest possibility is to assume that the copolymer consists of a single layer; this was found to fit the data of Figure 2 reasonably satisfactorily, and Figure 3 shows the derived surface excesses and layer thicknesses based on this simple model. Qualitatively, the level of the reflected signal depends on the square of the coverage, and the decrease of reflectivity with κ is more rapid the thicker the layer. Thus, even without a quantitative fit, the abrupt change in the reflectivity profiles of Figure 2 with increasing concentration shows that there is a sudden increase in the thickness of the layer with increasing surface coverage. This is clearly confirmed by the parameters required to fit the reflectivity that are given in Table 1. There is a marked change in thickness between bulk copolymer concentrations of 0.1 and 0.2 wt %.

It is not possible to derive more detailed information about the structure of the layer, particularly its composition profile, without using other isotopic compositions. We used two other isotopic compositions, poly(DMAEMA-*b*-dMMA) in D_2O and poly(DMAEMA-*b*-hMMA) in D_2O. For the latter, the signal from the copolymer is very weak and the reflectivity is dominated by the D_2O profile normal to the surface. If the copolymer is immersed to any significant extent, D_2O will be displaced and the reflectivity will be determined by the profile of the displaced water. Measurement of this profile therefore gives direct information about the immersion of the copolymer at the interface. In the case of the poly(DMAEMA-*b*-dMMA) in D_2O, the dMMA also contributes strongly to the reflectivity. To a first approximation, if the dMMA is in the region from which D_2O is displaced, the reflectivity from this isotopic composition will be higher than from poly(DMAEMA-*b*-hMMA) in D_2O. If the dMMA is out of the water it will have a more complicated effect, probably causing some interference effects in the reflectivity. Figures 4 and 5 respectively show the reflectivities of the copolymer at two compositions, 0.04 and 0.2 wt %, either side of the phase transition. At 0.04 wt %

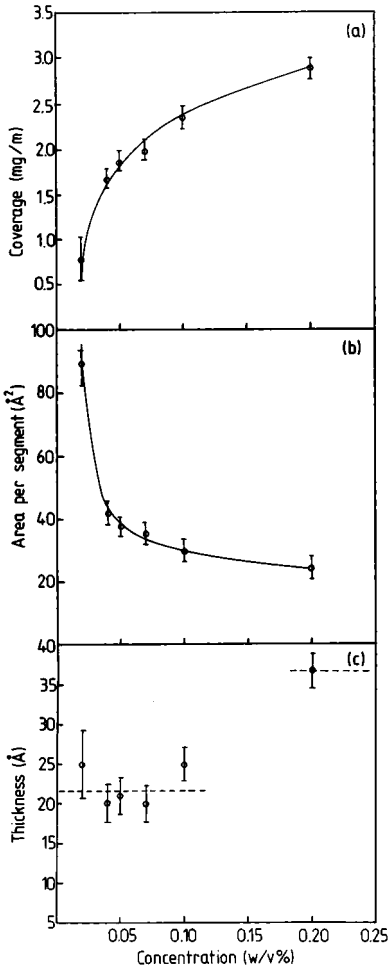

Figure 3. Variation of (a) coverage, (b) area per mean segment (defined as 1 MMA and 2 DMAEMA), and (c) thickness of copolymer layer with concentration as deduced from neutron reflection. The lines are only for guidance.

TABLE 1: Best Fits of a Single Uniform Layer to Neutron Reflectivities from Poly(DMAEMA-*b*-dMMA) in Null Reflecting Water

concn/ wt %	thickness/ Å	$\rho \times 10^6$/ Å^{-2}	Γ/mg m^{-2}	A per seg.^{b}/Å^2	polymer charge
0.02	20 ± 4	0.6	0.8	89	21
0.04	20 ± 3	1.6	1.7	42	11
0.05	21 ± 3	1.7	1.9	38	11
0.07	20 ± 2	1.9	2.0	35	11
0.1	25 ± 2	1.8	2.3	30	10
0.2	37^a	1.5	2.9	24	

^{a} Poor fit (see text). ^{b} Refers to the mean segment containing 1 MMA and 2 DMAEMA.

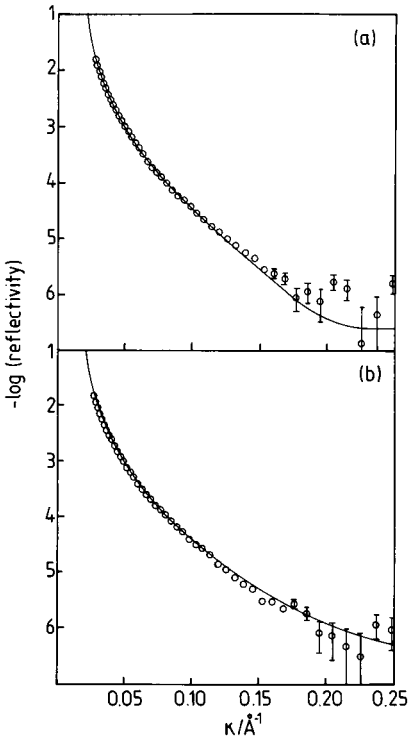

Figure 4. Neutron reflectivity profiles of (a) poly(DMAEMA-*b*-dMMA) and (b) poly(DMAEMA-*b*-hMMA) in D_2O at a concentration of 0.04 wt % at pH = 7.5. The continuous lines are the best fits using the parameters given in Table 3.

(Figure 4), the reflectivity profiles are significantly different from D_2O on its own, which shows that the layer is appreciably immersed in the aqueous subphase, and there is almost no difference between them, which shows that the MMA and DMAEMA components are extensively mixed. At the higher concentration of 0.2 wt % (Figure 5), the two D_2O reflectivity profiles are different from each other (Figure 5b,c), indicating that the MMA is not uniformly distributed throughout the layer, and they are both different from D_2O, indicating significant penetration of the subphase. The reflectivity of the partially deuterated material in D_2O at 0.2 wt % also falls off much more rapidly than that at 0.04 wt %, which further supports the earlier deduction that the layer is much thicker at 0.2 wt % (these reflectivity profiles are superimposed in Figure 6). The qualitative structural deductions given above are unambiguous and could not be interpreted in any other way. Quantitative fitting of the profiles, especially when the known stoichiometry of the polymers is taken into account, leads to a more precise structure.

The reflectivities in D_2O cannot be explained by the single-layer model used to fit the NRW data. There have to be at least two component layers, both containing some polymer but only one containing D_2O. The scattering-length density of any component layer can be expressed in terms of the volume fraction, ϕ_i, of the fragments constituting that layer

$$\rho = \phi_M\rho_M + \phi_D\rho_D + \phi_W\rho_W \qquad (3)$$

where M denotes the MMA fragment, D the DMAEMA fragment, and W water. When there is more than one component layer, special care must be taken to preserve the stoichiometry of the polymer and to conform to space-filling constraints, which requires an approximate knowledge of the volumes, of the three components. There is some uncertainty in the specific volumes, and this and possible isotopic differences can contribute errors or make it difficult to fit one chemical

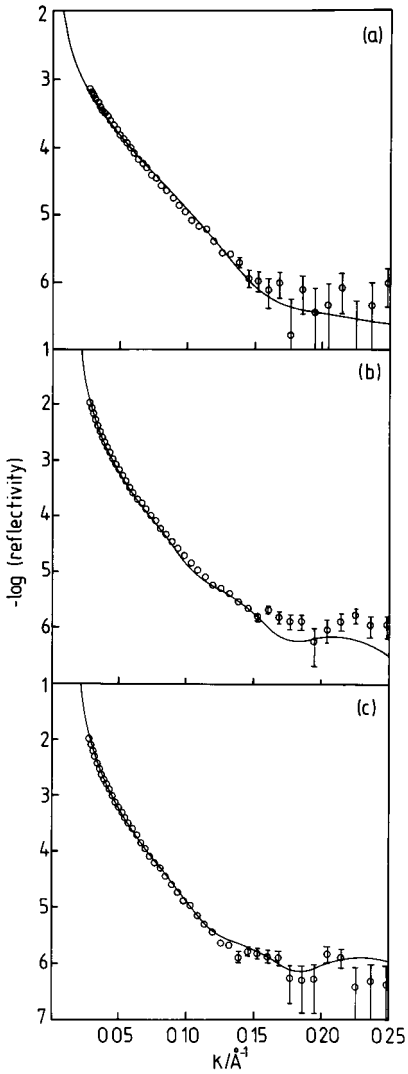

Figure 5. Neutron reflectivity profiles of (a) poly(DMAEMA-*b*-dMMA) in NRW, (b) poly(DMAEMA-*b*-dMMA) in D_2O, and (c) poly-(DMAEMA-*b*-hMMA) in D_2O at a concentration of 0.2 wt % at pH = 7.5. The continuous lines are the best fits using the parameters given in Table 3.

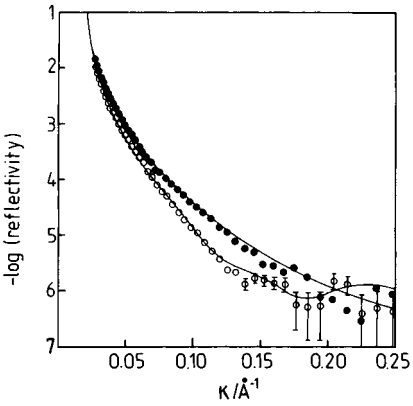

Figure 6. Comparison of the neutron reflectivities of the fully protonated copolymer in D_2O at 0.04 (●) and 0.2 wt % (○).

structure to the set of reflectivities from the different isotopes. The scattering lengths, volumes, and scattering-length densities of the three components of the interface that were used in the analysis are given in Table 2. Since the D_2O profiles require a minimum of two layers even to account qualitatively for the observed reflectivity, we started by attempting to fit a two-layer

TABLE 2: Volumes and Scattering Lengths for Copolymer Fragments

unit	volume/Å^3	scattering length $\times 10^5$ Å	scattering-length density $\times 10^6$/Å^{-2}
MMA-h_9	140[a]	14.92	1.07
MMA-d_9	140[a]	98.24	7.02
DMAEMA	225[a]	17.98	0.80
H_2O	29.9	−1.68	−0.56
D_2O	30.2	19.14	6.34

[a] See ref 27.

model simultaneously to the three reflectivity profiles from the different isotopic compositions and, if this was unsuccessful, then to fit three, four layers, etc. Note that although a one-layer model satisfactorily accounts for the reflectivity of the deuterated copolymer in NRW at 0.04 wt % and a two-layer model gives the best fit for the same contrast at 0.2 wt %, the requirement of the same chemical structure for different isotopes necessitated refitting these profiles with the same model as for the D_2O runs. Thus, with only the NRW data it would not be possible to deduce the more complicated structures that are necessary to fit the D_2O data. As with other systems of this type,[18,25] it was very difficult to find even one model that would fit all three reflectivity profiles! This difficulty gives us confidence that the structures that we eventually succeeded in fitting are unique within the estimated range of error. The calculated reflectivity profiles in Figures 2, 4, and 5 are for the parameters given in Table 2.

The structures of the layer at 0.04 and 0.2 wt % are completely different. Apart from the thickness difference, about which there can be no ambiguity from Figures 2 and 3, the structure within the layer is also quite different. The 0.04 wt % could be fitted with not less than two layers, but the 0.2 wt % required not less than four layers. The implications of this will be discussed in the next section, but here we give a brief discussion of the limitations of the fitted models. As indicated above, and as we have found in other neutron-reflection experiments on polymer monolayers, it is usually easy if the polymer is at least partially deuterated, to identify the position of the polymer in relation to the water. This is because for the fully protonated copolymer in D_2O the reflectivity depends on the thickness of the region from which water is displaced and the volume fraction of water left in this layer. For the copolymer containing dMMA, the reflectivity profiles will be completely different for the two cases where either the MMA block forms a separate layer out of the water or it is more or less uniformly mixed with the DMAEMA block. Given the particular stoichiometry, only the latter case can account for the small difference observed between the two profiles at 0.04 wt % shown in Figure 4 (they can be almost completely superimposed). Thus even without any model fitting to the data, the component layers for the 0.04 wt % layer must have similar compositions. Satisfactory quantitative fits were obtained over the range of compositions indicated by the errors given in Table 4, but the average is the identical composition given in the table. The observations that give rise to the particular structure identified for the 0.2 wt % solution are less easy to identify. The much greater thickness is clearly identified in the reflectivity profiles of the deuterated copolymer in NRW shown in Figure 2 and is therefore unambiguous. The large difference in the profiles of the 0.04 and 0.2 wt % solutions of poly(DMAEMA-*b*-dMMA) in D_2O in the middle range of κ, which we have superimposed in Figure 6, results from a higher volume fraction of polymer in the first two layers, but the more rapid decrease in reflectivity for the 0.2 wt % sample at low κ also shows that

TABLE 3: Best-Fitting Thicknesses and Scattering-Length Densities (ρ) for the Neutron Reflectivities from Three Isotopic Compositions of the Poly(DMAEMA-*b*-MMA)/Water System

		0.04 wt %	0.2 wt %
1st layer	thickness/Å	10	15
hD-dM/NRW	$10^6\rho_1$/Å^{-2}	1.6	1.0
hD-dM/D_2O	$10^6\rho_2$/Å^{-2}	1.6	1.0
hD-hM/D_2O	$10^6\rho_3$/Å^{-2}	0.6	0.7
2nd layer	thickness/Å	10	9
hD-dM/NRW	$10^6\rho_1$/Å^{-2}	1.6	2.5
hD-dM/D_2O	$10^6\rho_2$/Å^{-2}	2.8	2.5
hD-hM/D_2O	$10^6\rho_3$/Å^{-2}	1.8	0.7
3rd layer	thickness/Å		25
hD-dM/NRW	$10^6\rho_1$/Å^{-2}		0.8
hD-dM/D_2O	$10^6\rho_2$/Å^{-2}		5.0
hD-hM/D_2O	$10^6\rho_3$/Å^{-2}		4.5
4th layer	thickness/Å		30
hD-dM/NRW	$10^6\rho_1$Å^{-2}		0.0
hD-dM/D_2O	$10^6\rho_2$/Å^{-2}		5.8
hD-hM/D_2O	$10^6\rho_3$/Å^{-2}		5.8

TABLE 4: Composition of Poly(DMAEMA-*b*-MMA) Layers at the Air/Water Interface

		0.04 wt %	0.2 wt %
1st layer	thickness/Å	10 ± 2	15 ± 2
	ϕ_{MMA}	0.2 ± 0.02	0.05 ± 0.02
	ϕ_{DMAEMA}	0.6 ± 0.15	0.82 ± 0.15
	ϕ_{water}	0	0
2nd layer	thickness/Å	10 ± 2	9 ± 2
	ϕ_{MMA}	0.2 ± 0.02	0.3 ± 0.03
	ϕ_{DMAEMA}	0.6 ± 0.1	0.5 ± 0.15
	ϕ_{water}	0.2 ± 0.1	0.0 ± 0.1
3rd layer	thickness/Å		25 ± 4
	ϕ_{MMA}		0.09 ± 0.02
	ϕ_{DMAEMA}		0.21 ± 0.05
	ϕ_{water}		0.7 ± 0.1
4th layer	thickness/Å		30 ± 5
	ϕ_{MMA}		0
	ϕ_{DMAEMA}		0.1 ± 0.04
	ϕ_{water}		0.9 ± 0.1

a much larger thickness, relatively low volume fraction of polymer is also present. There is a relatively larger difference between deuterated and protonated polymers in D_2O than for the low concentration data, but it is still not very large; it is these two observations that support the interpretation that the MMA is out of the water but not as a layer on its own. Finally, the minimum number of layers required to fit the data for the 0.2 wt % sample was four. It is important to emphasize the key role of the stoichiometry of the copolymer in the determination of both structures. Neutron reflection from the partially deuterated species in NRW defines the MMA coverage accurately and unambiguously, and stoichiometry then defines the DMAEMA coverage accurately. Without constraining the fits to the correct stoichiometry, it would be undoubtedly be possible to fit the reflectivity data with a smaller number of layers, but they would not be consistent with the correct formula. The interplay between stoichiometry and the layer structure has been discussed in full detail in an earlier paper.[25] Alternative structures could have used to fit the data but with roughness between the layers. The main effect of including roughness between two layers is that it is approximately equivalent to changing from a two-layer to a three-layer model with the additional intervening layer having a composition intermediate between the two bounding layers and the overall thickness staying the same; i.e., it smooths the rather abrupt divisions characteristic of the use of a small number of layers. Although this would have some effect on the calculated profiles, our experience is that, at the relatively low values of κ used in

neutron reflectivity, its effects are small and do not justify the large number of extra fitting parameters. The estimated errors in Table 4 do, however, make allowance for the effects of roughness on the parameters given. External roughness of the layer, resulting from capillary waves, would be expected to have a very small effect on the profiles in this range of κ.

Finally, we note that specular neutron reflection gives no information about the lateral structure of the monolayer. It sees the layers as uniform in the plane provided that the dimensions of any in-plane inhomogeneities are smaller than the coherence length of the experiment, which is of the order of micrometers. Given that the structure of the layer at 0.2 wt % somewhat resembles the expected cross section of a distorted micelle, it seems possible that there may be lateral structure with micellar dimensions. This would not be detected. We have attempted to observe off-specular reflection from the system, but any signal is apparently too small to be detected above the relatively high incoherent scattering background.

Discussion

We have shown in an earlier paper that, with an independent determination of the surface excess, it is possible to use the Gibbs equation to determine the degree of ionization of a similar adsorbed copolymer in concentration regions where there is no association of the copolymer in the bulk. The full expression for the Gibbs equation may be written[18]

$$-\frac{d\gamma}{RT} = \Gamma_{pol}\, d \ln f_{pol}c_{pol} + \Gamma_{ion}\, d \ln f_{ion}c_{ion} + \Gamma_{coion}\, d \ln f_{coion}c_{coion} \quad (4)$$

where Γ represents surface excess (measured relative to water), c is concentration, f is activity coefficient, and the subscripts refer to copolymer, counterion, and co-ion. When the copolymer is the only source of counterions and the surface is neutral, then if we assume that the copolymer charge is the same in solution and at the surface, the equation becomes

$$-\frac{d\gamma}{RT} = \Gamma_{pol}(1+n)\, d \ln c_{pol} + \Gamma_{pol}\, d\, n + \Gamma_{pol}(d \ln f_{pol} + n\, d\, f_{ion}) \quad (5)$$

where n is the total charge on an average copolymer chain and Γ_{pol} is the true adsorbed amount. In the concentration range where the copolymer does not form aggregates in the bulk solution, n should be constant at a given pH. Neglecting any contribution from variation of the activity coefficients with concentration the Gibbs surface excess Γ_G will be given by

$$\Gamma_G \approx \Gamma_{pol}(1+n) \quad (6)$$

Taking the set of values of Γ_{pol} from the neutron measurements and Γ_G from the slope of the surface tension curve of Figure 1 at the appropriate concentration gives the set of values of n given in the last column of Table 1. Apart from the very lowest concentration, where the determination of the Gibbs slope is likely to be the least acccurate, the average value of n gives a fractional charge on the polymer of 0.23 ± 0.05. In the derivation of eq 5, n is basically the number of adsorbed counterions on a single copolymer chain at the surface and is therefore a measure of the number of ionized groups, DMAEMAH$^+$, per copolymer chain. Use of the simple equation

$$pK_a = \log\frac{[BH^+]}{[B]} + pH \quad (7)$$

gives a pK_a value of 6.8 at the surface. This is slightly lower than the value given by Hoogeveen et al. of ca. 7−7.5.[5] This may indicate that the effective K_a is lower at the surface, but since Hoogeven et al. give no detail of the derivation of their value we defer discussion of the possibility of any difference between surface and bulk pK_a to a later paper. We have only included the determination of the surface charge to assist in the following discussion of the structure.

The structures observed at both concentrations are somewhat unexpected in that there is no clear division into a hydrophobic buoy-tethered chain type of structure, which is what is usually assumed for diblock copolymers at interfaces. The DMAEMA residues are clearly acting both as hydrophobic and as hydrophilic units. At 0.04 wt % copolymer about half of the DMAEMA block is out of the water and at 0.2 wt % about two-thirds is out of the subphase. It seems unlikely that any charged DMAEMA residues would be out of the water layer, although Li et al.[3] in a study of spread poly(styrene-*b*-*N*-alkylvinylpyridinium iodide) (PS-*b*-PVP$^+$I$^-$) found no water at all in their spread monolayers, i.e., all the charged polymer residues were present with their counterions without any water molecules. If the charges were uniformly distributed throughout the DMAEMA block, the average charge would be associated with one charged and three uncharged DMAEMA residues. Because uncharged DMAEMA residues will be strongly surface active, possibly even more surface active than the MMA residues, this partially ionized unit will itself be powerfully surface active with the uncharged groups acting as a buoy and the charged groups embedded in the aqueous subphase. Thus in the absence of any constraints on the polymer backbone and any interactions (presumably favorable) between the similar DMAEMA and MMA fragments, all of the MMA and three-quarters of the DMAEMA would form the hydrophobic layer. There are several problems with such a structure; the copolymer backbone would be confined to a plane at, or just above, the surface of the water, which would be entropically unfavorable, the density of the hydrophobic layer would be unrealistically high, interactions between the similar DMAEMA and MMA fragments would probably act so as to cause some mixing of these two components, and part of the uncharged DMAEMA molecule also interacts favorably with water. The first factor will tend to thicken the layer, the first three factors will all lead to DMAEMA/MMA mixing, and the last will cause a greater penetration of the layer by water. Given these considerations, the observed structure of a completely mixed layer half-immersed in water, which is approximately what we observe at a concentration of 0.04 wt % polymer, is not unreasonable.

In the above discussion we have assumed that the layer is homogeneous in the plane of the interface, but this is not certain because the neutron specular reflection experiment gives no indications one way or the other. If the layer were nonuniform for the 0.04% solution, it would imply that backbone entropy required some separation of MMA and DMAEMA, that favorable interaction between the DMAEMA and MMA residues was not an important factor, or that the partially charged DMAEMA block actually causes phase separation of DMAEMA and MMA. If there were phase separation to give MMA-rich and DMAEMA-rich domains, the structure given in Table 4 would require the two domains to be at the same level in the interface and both to be half-immersed in the water. While such a structure is not impossible, it would seem unlikely that the MMA block could be even slightly immersed in the water subphase, as is required by the model in Table 4.

The possibility that the layer is not uniform in the plane would

be more significant for the 0.2% layer structure. The cross-sectional structure shows that the MMA block is not distributed at all uniformly in the layer, and it is tempting to assume that the second layer down, which contains about half of the MMA residues, is related to the core of an adsorbed micelle. If this layer is not uniform in the plane, the core could be extremely MMA-rich with the DMAEMA residues in the corona. The average composition of this layer could then be as observed. The general cross section of the layer is consistent with the adsorption of distorted micelles with the upper layers collapsed by dehydration and the lower layers extended into the aqueous solution. A significant fraction of the DMAEMA block, about two-thirds, is in the dehydrated regions, and these groups could either be uncharged or be present in an ion pair with their counterion. Li et al. found quite conclusively that with their copolymer ion pairs were present in a layer completely out of the water. We cannot tell one way or the other from our data. Note that there is no requirement that the value of the charge on the adsorbed copolymer, *n*, determined above, be the same for the two surface structures at 0.04 and 0.2 wt %, so there is therefore no reason there should not be fewer counterions associated with each copolymer molecule in the high-concentration layer in comparison with the low-concentration layer.

It is interesting to compare the dimensions of what appears to be a distorted micelle adsorbed at the surface with the dimensions of the copolymer in solution. For copolymer samples of comparable size and composition, dynamic light scattering experiments give a hydrodynamic radius in the region 100−135 Å.[8] The region in the surface layer that would correspond to the corona of the micelle is the lower two layers (see Tables 3 and 4) with a total thickness of about 55 Å. The core would correspond to the second layer, which is the layer richest in MMA, and this has a thickness of about 10 Å. The outer layer should just correspond to a flattened corona. Thus the estimated dimension of the fully solvated micelle, based on considering the surface as a flattened micelle, would be $(10 + 2 \times 55) = 120$ Å, which falls in the middle of the range estimated for the copolymer micelles in bulk solution. This is further support for the hypothesis that we are observing adsorption of micelles at the surface.

That adsorption of a soluble diblock copolymer occurs in the micellar form above a certain concentration is a phenomenon that is not observed for small-molecule surfactants. Nevertheless, small-molecule surfactants show a break in the surface tension vs ln *c* curves, which is used to identify the critical micelle concentration, the break being cause by a sudden change in the activity coefficient brought about by aggregation in the bulk solution. For the diblock copolymer the present results show that there could now be two breaks in the surface tension vs ln *c* plot, one corresponding to the change in activity resulting from bulk aggregation and one corresponding to a change in surface structure. These two changes need not occur at the same concentration, and indeed Dan and Tirrell have suggested that they might not coincide.[7] Unfortunately, the precision with which either transition can be measured is not sufficient to distinguish them in the present case.

Given the marked difference in structure of the monolayer at low and high concentrations, it is probable that the mechanism of formation of the monolayer is also quite different. At low concentrations, it is probable that the layer is built up by adsorption of the unimer, but, at high concentration, it is difficult to imagine that such a complex distribution of polymer in the direction of the surface normal could be created other than by adsorption of micelles, followed by drainage of water from the outer layer. A similar conclusion, that whole micelles are adsorbed, has been reached to explain the in-plane heterogeneity in layers of poly(styrene-*b*-vinylpyridinium salt) deposited on silicon or micas.[26]

Acknowledgment. F.L.B. thanks the School of Chemistry, Physics and Environmental Science, University of Sussex, and Courtaulds Research for financial support in the form of a D.Phil. studentship. S.P.A. and N.C.B. acknowledge EPRSC (formerly the SERC) for continued support of their water-soluble polymers research program at Sussex. R.K.T. also thanks EPSRC for support.

References and Notes

(1) Zhu, J.; Eisenberg, A.; Lennox, R. B. *Macromolecules* **1992**, *25*, 6547, 6556.
(2) Zhang, L. F.; Barlow, R. J.; Eisenberg, A. *Macromolecules* **1995**, *28*, 6055.
(3) Li, Z.; Zhao, W.; Quinn, J.; Rafailovich, M. H.; Sokolov, J.; Lennox, R. B.; Eisenberg, A.; Wu, X. Z.; Kim, M. W.; Sinha, S. K.; Tolan, M. *Langmuir* **1995**, *11*, 4785.
(4) Moffitt, M.; Khougaz, K.; Eisenberg, A. *Acc. Chem. Res*. **1996**, *29*, 95.
(5) Hoogeveen, N. G.; Cohen Stuart, M. A.; Fleer, G. J. *Faraday Discuss*. **1994**, *98*, 161.
(6) Wittmer, J.; Joanny, J. F. *Macromolecules* **1993**, *26*, 2691.
(7) Dan, N.; Tirrell, M. *Macromolecules* **1994**, *26*, 4310.
(8) Baines, F. L.; Armes, S. P; Billingham, N. C.; Tuzar, Z. *Macromolecules* **1996**, *29*, 8151.
(9) Richards, R. W.; Rochford, B. R.; Webster, J. R. P. *Faraday Discuss*. **1994**, *98*, 263.
(10) Gissing, S. K.; Richards, R. W.; Rochford, B. R. *Colloid Surf.* **1994**, *86*, 171.
(11) Richards, R. W.; Rochford, B. R.; Webster, J. R. P. *Polymer* **1997**, *5*, 1169.
(12) Bijsterbosch, H. D.; de Haan, V. O.; de Graaf, A. W.; Mellerna, M.; Leermakers, F. A. M.; Cohen-Stuart, M. A.; van Well, A. A. *Langmuir* **1995**, *11*, 4467.
(13) Hodge, P.; Towns, C. R.; Thomas, R. K.; Shackleton, C. *Langmuir* **1992**, *8*, 585.
(14) Phipps, J. S.; Richardson, R. M.; Cosgrove, T.; Eaglesham, A. *Langmuir* **1993**, *9*, 3530.
(15) Dai, L.; White, J. W.; Kerr, J.; Thomas, R. K.; Penfold, J.; Aldissi, M. *Synth. Met.* **1989**, *28*, 69.
(16) White, J. W.; Kerr, J. C. D.; Penfold, J.; Saville, P. M.; Thomas, R. K. *Progress in Pacific Polymer Science*; Ghiggino, Ed.; Springer-Verlag: Berlin, 1994; p 99.
(17) Kent, M. S.; Lee, L. T.; Farnoux, B.; Rondelez, F. *Macromolecules* **1992**, *25*, 6240.
(18) Su, T. J.; Styrkas, D. A.; Thomas, R. K.; Baines, F. L.; Billingham, N. C.; Armes, S. P. *Macromolecules* **1996**, *29*, 6892.
(19) Beadle, P. M.; Rowan, L.; Mykytiuk, J.; Billingham, N. C.; Armes, S. P. *Polymer* **1993**, *34*, 1561.
(20) Webster, O. W.; Hertler, W. R.; Sogah, D. Y.; Farnham, W. B.; Ranjanbabu, T. V. *J. Am. Chem. Soc*. **1983**, *105*, 5706.
(21) Penfold, J.; Ward, R. C.; Williams, W. G. *J. Phys. E* **1987**, *20*, 1411.
(22) Bucknall, D. G.; Penfold, J.; Webster, J. R. P.; Zarbakhsh, A.; Richardson, R. M.; Rennie, A. R.; Higgins, J. S.; Jones, R.; Fletcher, P. D.; Thomas, R. K.; Roser, S. J.; Dickinson, E. *SURF*; International Conference on Advanced Neutron Sources XIII, in press.
(23) Lu, J. R.; Simister, E. A.; Thomas, R. K.; Penfold, J. *J. Phys. Chem.* **1993**, *97*, 13907.
(24) Born, M; Wolf, E. *Principles of Optics*; Pergamon Press: Oxford, 1970.
(25) Styrkas, D. A.; Thomas, R. K.; Adib, Z. A.; Davis, F.; Hodge, P.; Liu, X. H. *Macromolecules* **1994**, *27*, 5504.
(26) Meiners, J. C.; Ritzi, A.; Rafailovich, M. H.; Sokolov, J.; Mlynek, J.; Krausch, G. *Appl. Phys.* **1995**, *A61*, 519.
(27) van Krevelen, P. W. *Properties of Polymers-their Correlation with Chemical Structure; their Numerical Estimation from Additive Group Contributions*, 3rd ed.; Elsevier: Amsterdam, 1990.